ACS OMEGA

Open Access

http://pubs.acs.org/journal/acsodf

Article

Monkeypox Virus Crosstalk with HIV: An Integrated Skin Transcriptome and Machine Learning Study

Xueyao Cai,[⊥] Tianyi Zhou,[⊥] Wenjun Shi, Yuchen Cai,* and Jianda Zhou*

Cite This: *ACS Omega* 2023, 8, 47283−47294

Read Online

ACCESS | Metrics & More | Article Recommendations | Supporting Information

ABSTRACT: The emergence of the monkeypox virus (MPXV) outbreak presents a formidable challenge to human health. Emerging evidence suggests that individuals with HIV have been disproportionately affected by MPXV, with adverse clinical outcomes and higher mortality rates. However, the shared molecular mechanisms underlying MPXV and HIV remain elusive. We identified differentially expressed genes (DEGs) from two public data sets, GSE219036 and GSE184320, and extracted common DEGs between MPXV and HIV. We further performed gene ontology (GO), Kyoto Encyclopedia of Genes and Genomes (KEGG), protein−protein interactions (PPI), candidate drug assessment, and immune correlation of hub genes analysis. We validated the key biomarkers using multiple machine learning (ML) methods including random forest (RF), t-distributed stochastic neighbor embedding (tSNE), and uniform manifold approximation and projection (UMAP). A total of 59 common DEGs were identified between MPXV and HIV. Our functional analysis highlighted multiple pathways, including the ERK cascade, NF-κB signaling, and various immune responses, playing a collaborative role in the progression of both diseases. The PPI and gene co-expression networks were constructed, and five key genes with significant immune correlations were identified and validated by multiple ML models, including SPRED1, SPHK1, ATF3, AKT3, and AKT1S1. Our study emphasizes the common pathogenesis of HIV and MPXV and highlights the pivotal genes and shared pathways, providing new opportunities for evidence-based management strategies in HIV patients co-infected with MPXV.

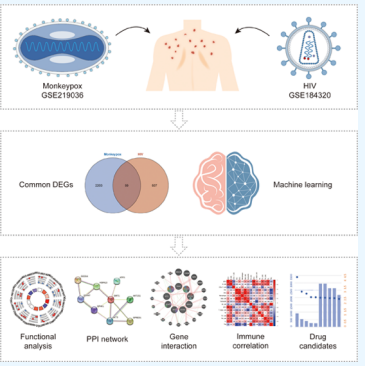

INTRODUCTION

As the world continues to fight against the ongoing COVID-19 pandemic, the World Health Organization (WHO) has officially declared the current outbreak of monkeypox (Mpox) virus (MPXV) a Public Health Problem of International Concern on July 23, 2022.[1] This zoonotic orthopox DNA virus, originating from a member of the Orthopoxvirus genus of the Poxviridae family, has been a cause of concern among humans since 1970.[2] While sporadic outbreaks of Mpox have been observed in Africa over the past half century, the recent near-simultaneous global outbreaks affecting more than 100 countries have generated significant alarm.[3] The clinical manifestation of this virus is characterized by fever, rash, and lymphadenopathy. Potential complications of Mpox infections include pneumonitis, encephalitis, sight-threatening keratitis, and secondary bacterial infections.[4,5] In contrast to previous outbreaks, the current Mpox epidemic is believed to spread through close contact or sexual contact, resulting in predominantly localized lesions instead of extensive disseminated lesions.[6,7] Despite the availability of Mpox vaccines, rapidly evolving mutant strains and the challenges associated with vaccine deployment to meet global demand have made the fight against MPXV a highly complex and demanding endeavor.

Acquired immune deficiency syndrome (AIDS) is a severe autoimmune disorder caused by human immunodeficiency virus (HIV) infection, characterized by persistent depletion of CD4+ T cells resulting in progressive immunodeficiency, opportunistic diseases, and mortality.[8] Similar to MPXV, HIV is spread through sexual contact and is more prevalent among men who engage in male−male sexual behavior. Previous studies have shown that individuals infected with HIV are disproportionately affected by the MPXV, accounting for 38−50% of people diagnosed with Mpox.[2] There is compelling evidence that most Mpox cases were in people who had high CD4 cell counts and similar outcomes to those without HIV.[9] Despite the relatively small number of individuals identified with HIV and MPXV co-infections, emerging data has indicated that such co-infections may lead to worse clinical outcomes and higher mortality rates.[10,11] A comprehensive understanding of the intricate interplay between MPXV and HIV is essential to providing novel insights into the common pathogenesis and facilitating the development of evidence-based management strategies in patients infected with both viruses.

Received: October 3, 2023
Revised: November 13, 2023
Accepted: November 14, 2023
Published: November 29, 2023

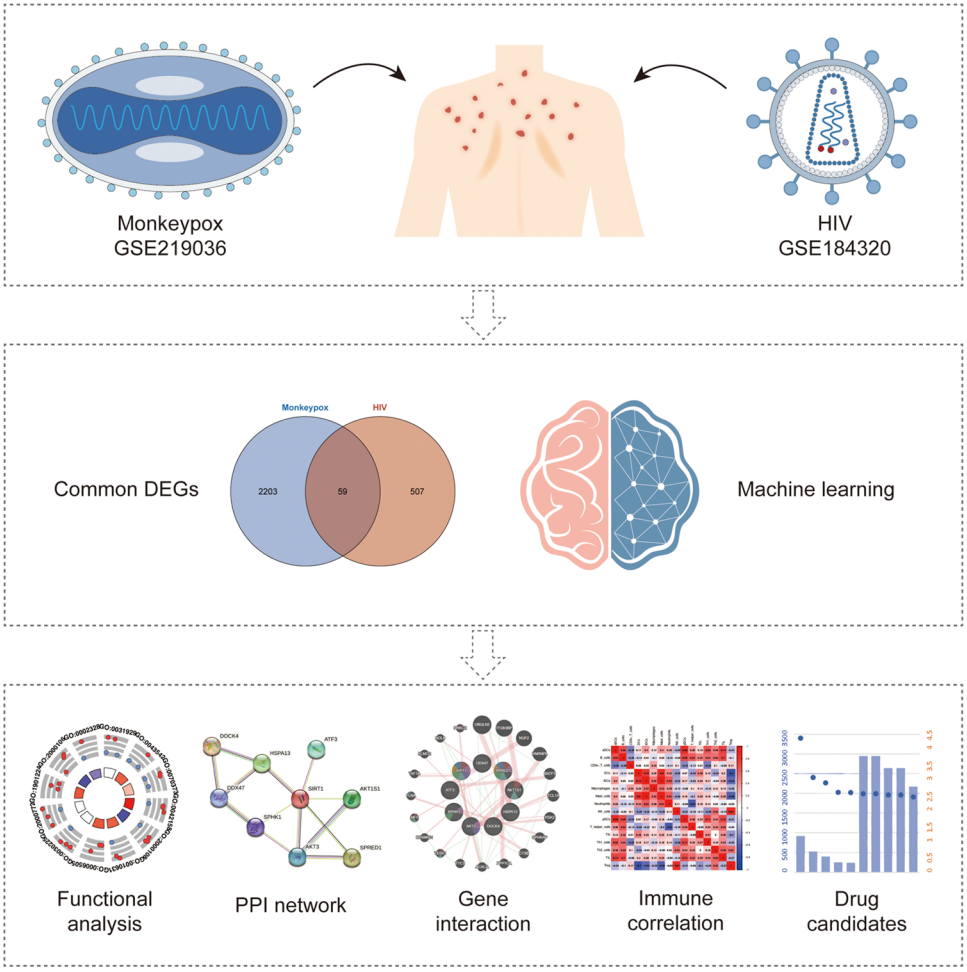

Figure 1. Schematic illustration of the present study.

The aim of our study was to identify the potential mechanism and therapeutic targets that may assist in the treatment of individuals with HIV and MPXV skin co-infection. Based on systematic bioinformatics approaches, we identified 59 common differentially expressed genes (DEGs) associated with HIV and MPXV, followed by enrichment analyses for functional explorations. We analyzed the protein−protein interactions (PPI), drug candidates, and immune correlation of the hub genes. Using multiple machine learning (ML) methods, including random forest (RF), t-distributed stochastic neighbor embedding (tSNE), and uniform manifold approximation and projection (UMAP), we validated the key biomarkers for the combined MPXV and HIV characterization. A schematic illustration of the general study procedures is depicted in Figure 1.

RESULTS

Identification of Common DEGs between MPXV and HIV. From the HIV data set GSE184320, a total of 566 DEGs were successfully identified. Specifically, 418 DEGs were found to be upregulated, while 148 DEGs were downregulated (Figure 2A). When comparing the MPXV data set GSE219036, a total of 2262 DEGs were identified. Of these, 1682 DEGs were upregulated and 580 DEGs were downregulated in MPXV-infected keratinocytes compared to mock-infected controls (Figure 2B). Following a comparative analysis, it was revealed that 59 DEGs were commonly expressed across both data sets (Figure 2C, Table S1).

Functional Enrichment Analysis. To elucidate the biological pathways that were enriched in these common DEGs between MPXV and HIV, we conducted comprehensive GO and KEGG analyses (Figure 2D−G). In GO analysis, among BP, the common DEGs were primarily involved in TOR signaling, endothelial cell migration, negative regulation of ERK1 and ERK2 cascade, lipoprotein biosynthetic process, epithelial cell migration, GPI anchor metabolic process, regulation of cellular senescence, and different immune processes including positive regulation of leukocyte apoptotic process, macrophage differentiation, positive regulation of NIK/NF-kappaB signaling, regulation of leukocyte apoptotic process, and pro-B cell differentiation (Figure 2D and Table S2). The CC of DEGs was mainly enriched in the NSL complex, PML body, fibrillar collagen trimer, banded collagen fibril, uropod, and chromatin silencing complex (Figure 2E and Table S3). For MF, we found that these DEGs were active participants in protein phosphatase 2A binding, acyltransferase activity, ATP hydrolysis activity, phosphatase binding, calmodulin binding, and RNA helicase activity (Figure 2F and Table S4). As for KEGG analysis, it revealed that the common DEGs were mostly enriched in the following pathways: VEGF signaling pathway, longevity regulating pathway, Fc γ R-mediated phagocytosis, glucagon signaling pathway, AMPK signaling pathway, cell adhesion molecules (CAMs), phospho-

https://doi.org/10.1021/acsomega.3c07687
ACS Omega 2023, 8, 47283−47294

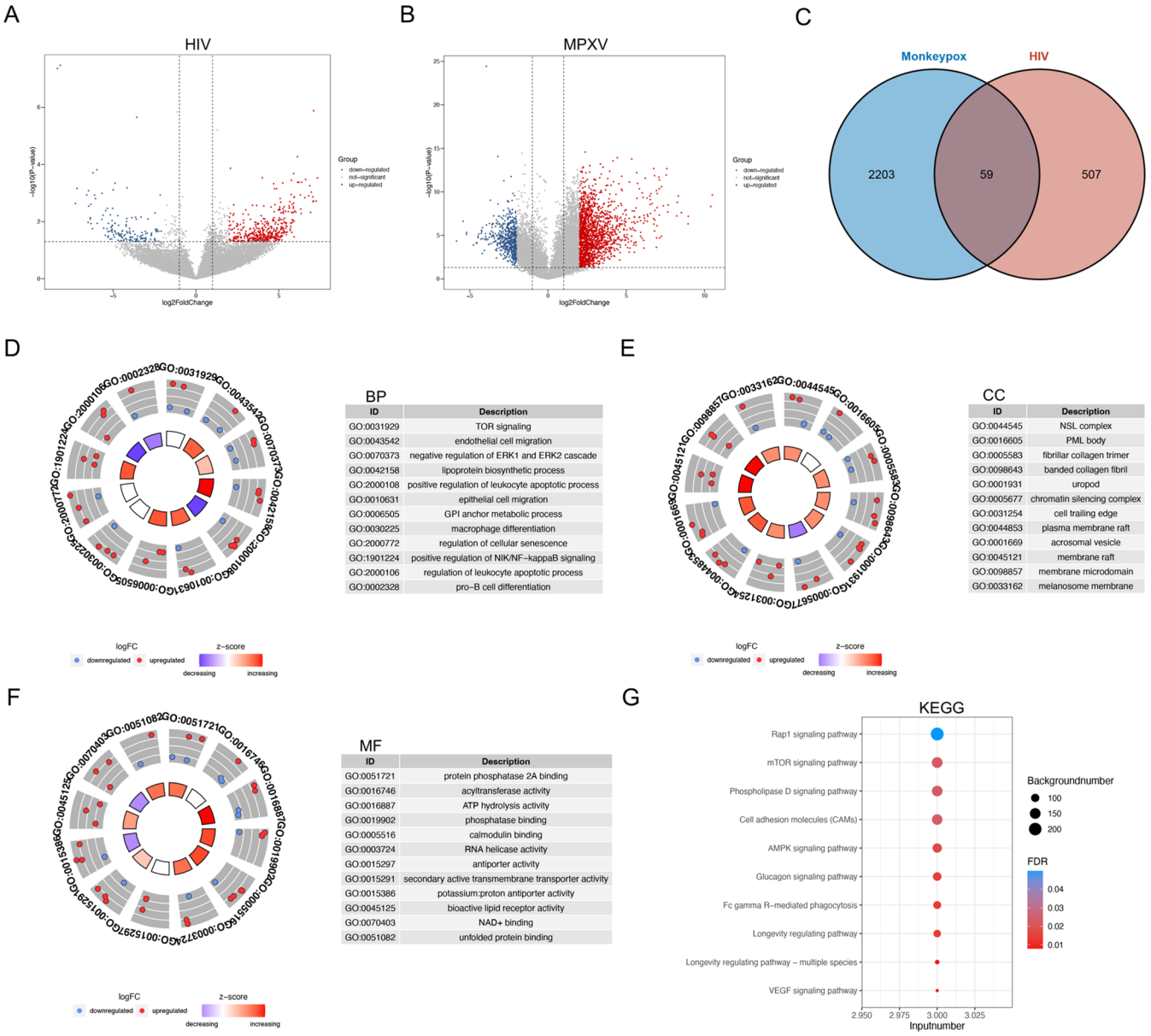

Figure 2. Identification of common differentially expressed genes (DEGs) between MPXV and HIV, and functional explorations. (A) Volcano plot showing 566 DEGs in the HIV data set GSE184320. (B) Volcano plot revealing 2262 DEGs in the MPXV data set GSE219036. (C) Venn graph showing an intersection of 59 common DEGs. Gene Ontology (GO) analysis of the common DEGs between MPXV and HIV, including (D) biological process (BP), (E) cellular component (CC), and (F) molecular function (MF). (G) Kyoto Encyclopedia of Genes and Genomes (KEGG) functional enrichment analysis of the common DEGs between MPXV and HIV.

lipase D signaling pathway, mTOR signaling pathway, and Rap1 signaling pathway (Figure 2G and Table S5). Altogether, our functional analyses demonstrated that multiple pathways, including the ERK cascade, NF-κB signaling, and various immune responses, play a collective role in the progression of both diseases.

Analysis of Hub Genes and Co-Expression Network. The PPI network was established by using the common DEGs identified through the STRING database and successfully visualized using Cytoscape. Employing a combined score threshold ≥0.4, a pivotal gene module was acquired, comprising 37 DEGs: IFIT2, HSPA13, PNPO, ATF3, STRN4, DOCK4, DDX47, DPM3, SPHK1, PSKH1, SELPLG, L1CAM, SPRED1, LY6K, PIGK, LIF, AKT3, ASB1, MRPL17, PLA2G4C, GORAB, MENG, PDCD1LG2, ZNF317, PARD6G, SIRT1, RAB2B, AKT1S1, PROCR, PTP4A3, PHKG2, CAPN15, HEATR3, TYRP1, COL5A2, APBA3, and FNIP1 (Figure 3A). Subsequently, a thorough screening process was conducted to identify common hub genes using seven algorithms including Closeness, MCC, Degree, MNC, Radiality, Stress, and EPC (Figure 3B). Through the intersection of Venn diagrams, a total of 9 common hub genes were successfully extracted, comprising DOCK4, DDX47, HSPA13, SPHK1, ATF3, SIRT1, AKT3, AKT1S1, and SPRED1 (Figure 3C). To construct a gene co-expression network, the 9 common hub genes were uploaded to the GeneMANIA database to decipher their correlations among co-expression, physical interactions, prediction, and genetic interactions. As a result, 20 predicted genes correlated with the 9 common hub genes were determined. All genes in this co-

https://doi.org/10.1021/acsomega.3c07687
ACS Omega 2023, 8, 47283−47294

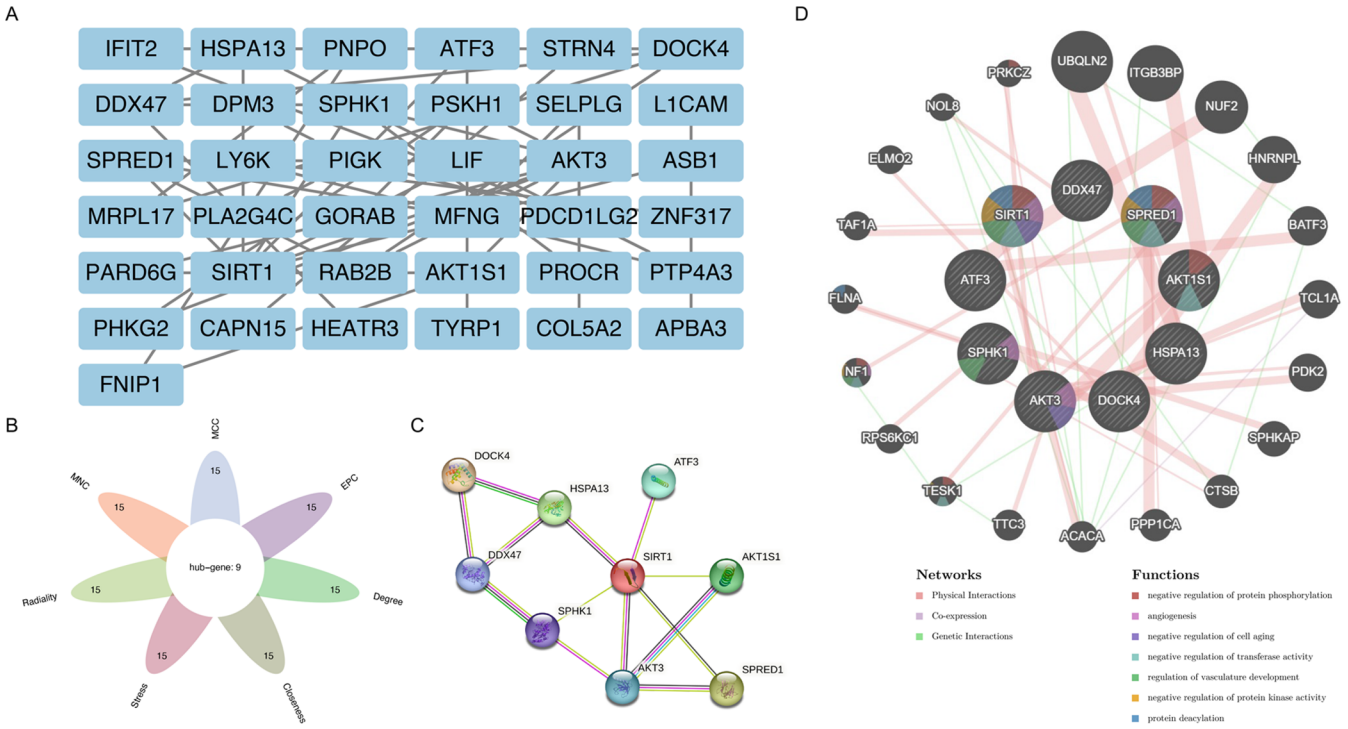

Figure 3. Analysis of hub genes extracted from the common DEGs between MPXV and HIV. (A) Key gene module showing 37 shared DEGs. (B) Venn diagram showing a total of 9 overlapping hub genes screened by seven algorithms. (C) Protein−protein interaction (PPI) network of the 9 hub genes drawn by the Cytoscape plug-in CytoHubba. (D) Hub genes and their co-expression genes interaction network analyzed by GeneMANIA.

expression network were mainly enriched in negative regulation of protein phosphorylation, angiogenesis, negative regulation of cell aging, negative regulation of transferase activity, regulation of vasculature development, negative regulation of protein kinase activity, and protein deacylation (Figure 3D).

Characteristics of Immune Correlation. Since functional analyses indicated that different immune responses participated collectively in the progression of MPXV and HIV, we aimed to investigate the exact role of immune cells and immune pathways in the development of both diseases. Using the HIV data set, we first performed the correlation analyses between the enrichment scores of immune cells (Figure 4A) and between the enrichment scores of immune functions (Figure 4B). The correlation matrix demonstrated that certain immunocytes (e.g., pDCs, TIL, B cells, and CD8+ T cells) were closely and positively correlated with other immune cells, implying their pivotal position in orchestrating immune responses during HIV pathogenesis (Figure 4A). In addition, we discovered that the HIV pathogenesis was influenced by numerous immune responses, especially the signaling pathways of CCR, checkpoint, HLA, and inflammation promotion (Figure 4B). We further conducted Pearson's correlation to analyze the correlation between the hub genes and distinct immune cells/pathways. As revealed in Figure 4C, a total of 5 genes (SPRED1, SPHK1, ATF3, AKT3, and AKT1S1) exhibited a significant correlation with various immune activities in HIV, which were defined as key genes for further analysis. Similarly, our investigation also revealed the crucial role of certain immune cells (e.g., aDCs, pDCs, mast cells, B cells, and Treg) and immune pathways (e.g., APC co-inhibition, CCR, checkpoint, HLA, inflammation-promoting, and T cell costimulation) in MPXV development (Figure 5A,B). Further Pearson's correlation suggested that all of these common hub genes played a pivotal role in MPXV (Figure 5C). Based on the above analysis, five key genes (SPRED1, SPHK1, ATF3, AKT3, and AKT1S1) were determined critical for the shared pathogenesis of HIV and MPXV. For the visualization of 5 key genes among different samples, we sketched the radar plots for the visualization of 5 key genes among different samples in the HIV (Figure 6A) and MPXV data set (Figure 6C). The correlation among the 5 key genes was also demonstrated in both HIV (Figure 6B) and MPXV data set (Figure 6D).

Biomarker Screening via Multiple Machine Learning Models. As shown in Figure 7A, following the identification of the 5 key genes (SPRED1, SPHK1, ATF3, AKT3, and AKT1S1), ATF3 and SPHK1 were further validated as the most promising biomarkers using the RF model, with remarkable predictive accuracy for HIV outcomes (Figure 7B). Similarly, we identified ATF3 and AKT1S1 upon performing an RF screen on the MPXV data set (Figure 7C,D). Based on the screen two genes ATF3 and SPHK1, a significant trend distinction between the HIV and healthy samples was observed using the tSNE (Figure 7E) and UMAP model (Figure 7F), indicating the excellent ability of these two genes in differentiating HIV patients from healthy individuals. Notably, in addition to the separation of MPXV and normal groups, the tSNE classified the MPXV samples into two distinct clusters, indicating the potential of the two genes for further characterization of MPXV subtypes (Figure 7G). A similar trend distinction was observed between the MPXV and healthy samples using the UMAP model (Figure 7H).

Identification of Candidate Drugs. In order to investigate the potential effects of pharmaceutical molecules on the common disease pathways, we used the DSigDB of

https://doi.org/10.1021/acsomega.3c07687
ACS Omega 2023, 8, 47283−47294

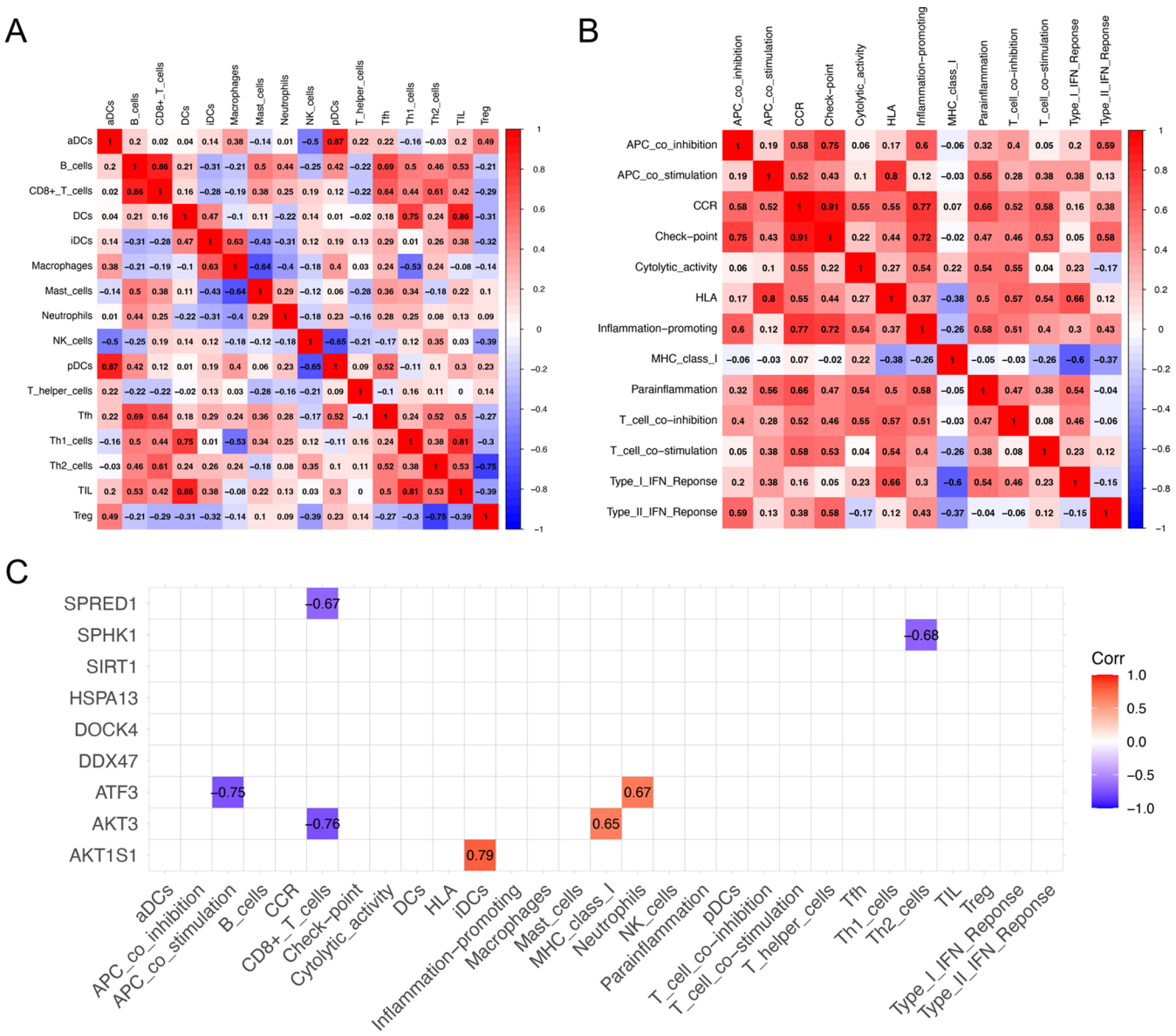

Figure 4. Landscape of immune correlation in HIV. (A) Correlation matrix of enrichment scores between the 16 immune cell types and (B) the 13 immune pathway proportions in HIV. (C) Matrix diagram showing the correlation between the 9 hub genes and the 16 immune cell types and 13 immune pathways. The correlation scores were presented on criteria of $p < 0.05$.

Enrichr website to conduct a pharmacological search for the 5 key genes. Based on their combined scores, the top 10 therapeutic compounds were selected for potential combined therapy, including Torcetrapib, L-leucine, Parthenolide, MG-262, 8-Azaguanine, Glyoxal, GSK690693, AR-A014418, Go 6976, and BMS-536924 (Figure 8 and Table S6).

DISCUSSION

The emergence of MPXV has cast a new pandemic to the world, posing a formidable challenge to global public health. Despite the accumulation of evidence indicating possible links between HIV and MPXV, the molecular and pathogenic connections underlying their co-infections remain poorly understood. To our knowledge, the present work is the first to demonstrate the shared pathogenesis of HIV and MPXV. In our study, we identified the shared DEGs and elucidated that multiple pathways, including ERK cascade, NF-κB signaling, and various immune responses, played a collaborative role in the progression of HIV and MPXV. By creating the PPI and co-expression network, we found 5 key genes with significant immune correlations. We validated the key biomarkers using multiple ML algorithms and suggested therapeutic drugs for combined therapy. In light of our findings, this study provides new insights into the shared relationship between HIV and MPXV.

In the present study, we have identified a total of 5 key genes with significant immune correlation, including SPRED1, SPHK1, ATF3, AKT3, and AKT1S1. Sprouty-related Ena/VASP homology 1 domain-containing protein 1 (SPRED1) functions as a suppressor of the Ras-ERK pathway and plays an essential role in multiple cytokine signalings and immune tolerance responses.[12,13] In addition, SPRED1 is a potential target for the regulation of hantavirus-induced human endothelial cell permeability.[14] Interestingly, SPRED1 plays a crucial role in mediating the crosstalk between ERK1/2 and Wnt/β-catenin pathways, thereby facilitating viral replication

https://doi.org/10.1021/acsomega.3c07687
ACS Omega 2023, 8, 47283−47294

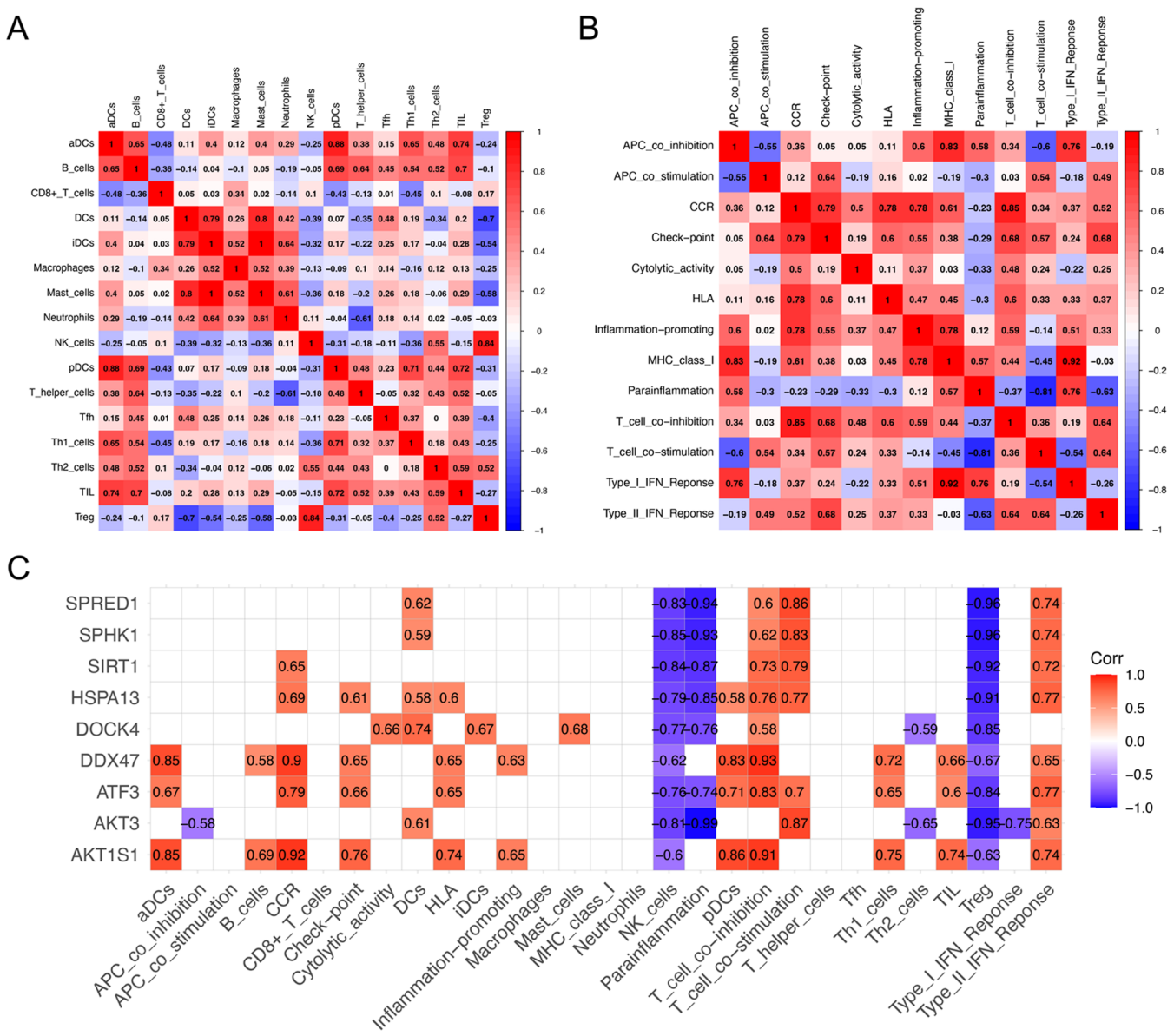

Figure 5. Landscape of immune correlation in MPXV. (A) Correlation matrix of enrichment scores between the 16 immune cell types and (B) the 13 immune pathway proportions in monkeypox. (C) Matrix diagram showing the correlation between the 9 hub genes and the 16 immune cell types and 13 immune pathways. The correlation scores were presented on criteria of $p < 0.05$.

and increasing viral cytopathogenicity.[15] The sphingosine kinase 1 (SphK1) enzyme participates in the phosphorylation of sphingosine to sphingosine 1-phosphate (S1P).[16] A growing body of evidence indicates that the SPHK/S1P axis is a crucial regulator of cellular activities during diverse viral infection processes.[17] Recent research demonstrates that inhibition of SphK1 could potentially reduce HIV-1 transmission, as observed in CD4+ T cells and macrophages. It is proposed that therapeutic targeting of SPHK or S1P receptors could potentially aid in the development of strategies to prevent establishment and transmission of HIV-1 infection among immune cells.[18] Activating transcription factor 3 (ATF3), a stress-induced transcription factor belonging to the ATF/cAMP response element-binding (CREB) family, plays an important role in regulating metabolism, immunity, and oncogenesis.[19] Being a key modulator of diverse inflammatory and immune activities, ATF3 is implicated in the antiviral signaling and autophagy in response to various viral infections, including hepatitis B virus, Japanese encephalitis virus, and HIV.[20−23] AKT, a protein kinase belonging to the AGC family, is a key effector of the phosphatidylinositol 3-kinase (PI3K) and regulates diverse cellular processes, including cell proliferation, cell survival, metabolism, and inflammation.[24] AKT3 is crucial for the regulation of cytokine release and immune activities.[25] Specific silencing of AKT3 resulted in a significant reduction in CCL5 production in astrocytes transfected with HIV-1 viral protein R.[26] Similarly, AKT1S1 was found to be one of the CXCL12-responsive AKT substrates implicated in the regulation of HIV-1 infection of T cells.[27] To conclude, all of these hub genes may serve as potential biomarkers for targeted therapies of HIV and MPXV co-infection. Further research into these genes is essential to advance our understanding of the underlying mechanisms of both diseases.

Previous studies have shown that the majority of MPXV cases were observed in individuals with high CD4+

https://doi.org/10.1021/acsomega.3c07687
ACS Omega 2023, 8, 47283−47294

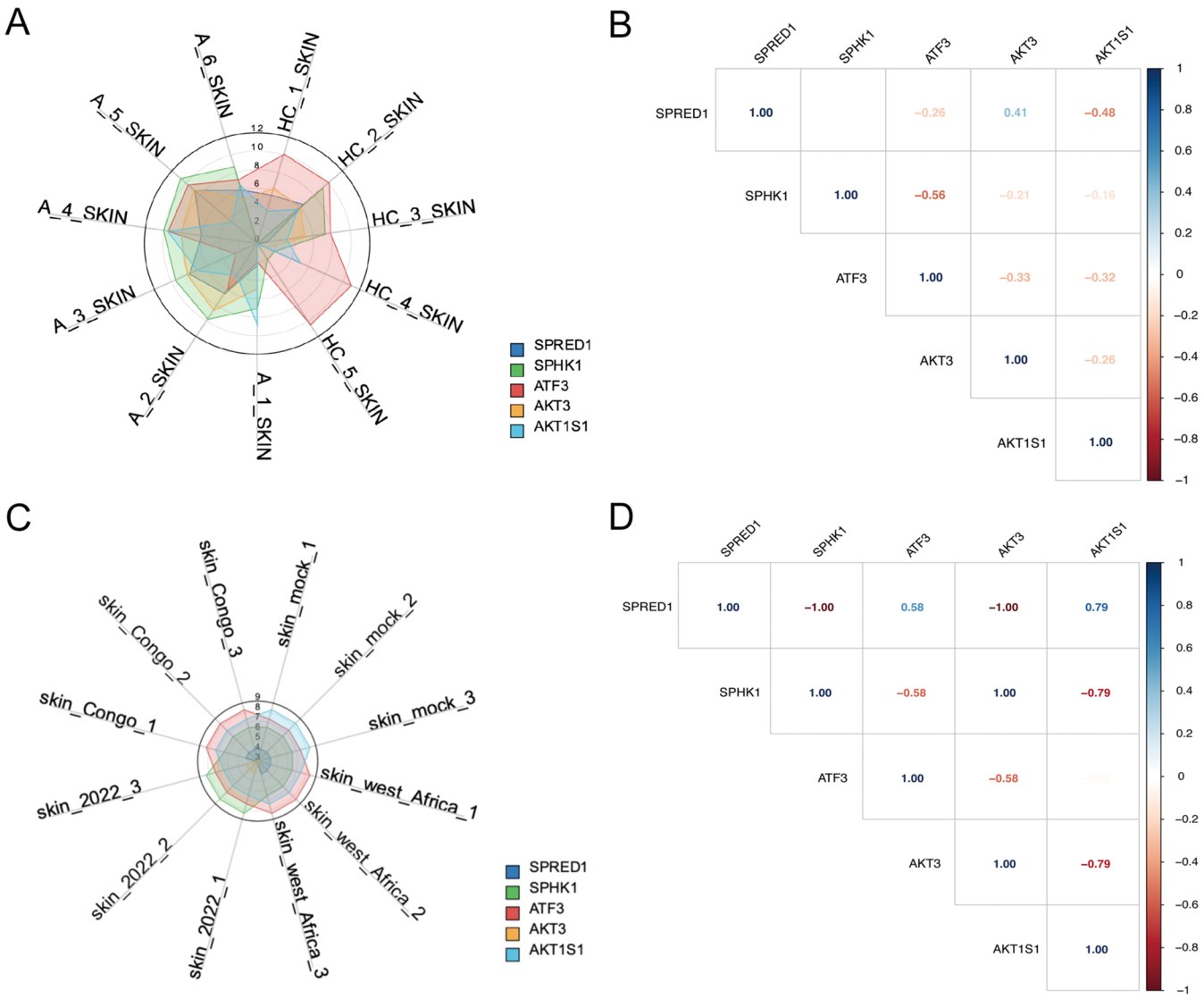

Figure 6. (A) Radar plot visualization of 5 key genes (SPRED1, SPHK1, ATF3, AKT3, and AKT1S1) among HIV samples. (B) Correlation among the 5 key genes demonstrated in the HIV data set. (C) Radar plot visualization of 5 key genes (SPRED1, SPHK1, ATF3, AKT3, and AKT1S1) among MPXV samples. (D) Correlation among the 5 key genes demonstrated in the MPXV data set.

lymphocyte counts compared to those without HIV, highlighting the pressing need for mechanistic studies to elucidate the impact of MPXV- and HIV-associated immunocompromise on infection acquisition and clearance. In this study, we investigated the functional associations between MPXV and HIV. The GO and KEGG analyses demonstrated that diverse immune responses and signaling pathways, such as the ERK cascade, NF-κB, and TOR signaling, play crucial roles in the pathogenesis of HIV and MPXV co-infection. The immunomodulatory ERK signaling plays a key role in the regulation of cytokines (IL-2, IL-10, and TNF-a) and biomarkers (PD-1 and Fas/FasL) that are skewed in chronic HIV infection.[28] Notably, ERK is also involved in the invasion and transmission of MPXV, providing a potential avenue for the treatment of the epidemic.[29] The NF-κB signaling pathway has long been recognized as a valuable target for HIV infection.[30] Recently, a plethora of individual compounds have been screened to activate HIV transcription via NF-kB signaling in vitro and ex vivo, providing a promising path forward for the development of alternative drug targets for HIV.[31,32] Additionally, using transcriptomic approach, researchers have identified the pivotal role of NF-κB signaling in MPXV infection in both monkey and human models.[33] Based on in silico structural and functional characterization, a hypothetical protein from MPXV, Q8 V4Q4, has been proposed to prevent host NF-kB activation in response to pro-inflammatory cytokines.[34] Our study provides significant insight into the molecular mechanisms underlying both HIV and MPXV co-infection, facilitating a better understanding of the disease mechanism and encouraging further exploration in future experiments.

Our exploration also included the possible pharmaceuticals that could potentially affect the common disease pathways including Torcetrapib, L-leucine, Parthenolide, MG-262, 8-azaguanine, Glyoxal, GSK690693, AR-A014418, Go 6976, and BMS-536924. Parthenolide, a naturally occurring sesquiterpene lactone derived from feverfew, exhibits a broad spectrum of antiparasitic, antiviral, and anti-inflammatory effects.[35,36] This agent can selectively inhibit the T cell receptor (TCR) activation, providing immunotherapeutic potentials for diverse virus infections, such as SARS-CoV-2 and HIV.[37] The

https://doi.org/10.1021/acsomega.3c07687
ACS Omega 2023, 8, 47283−47294

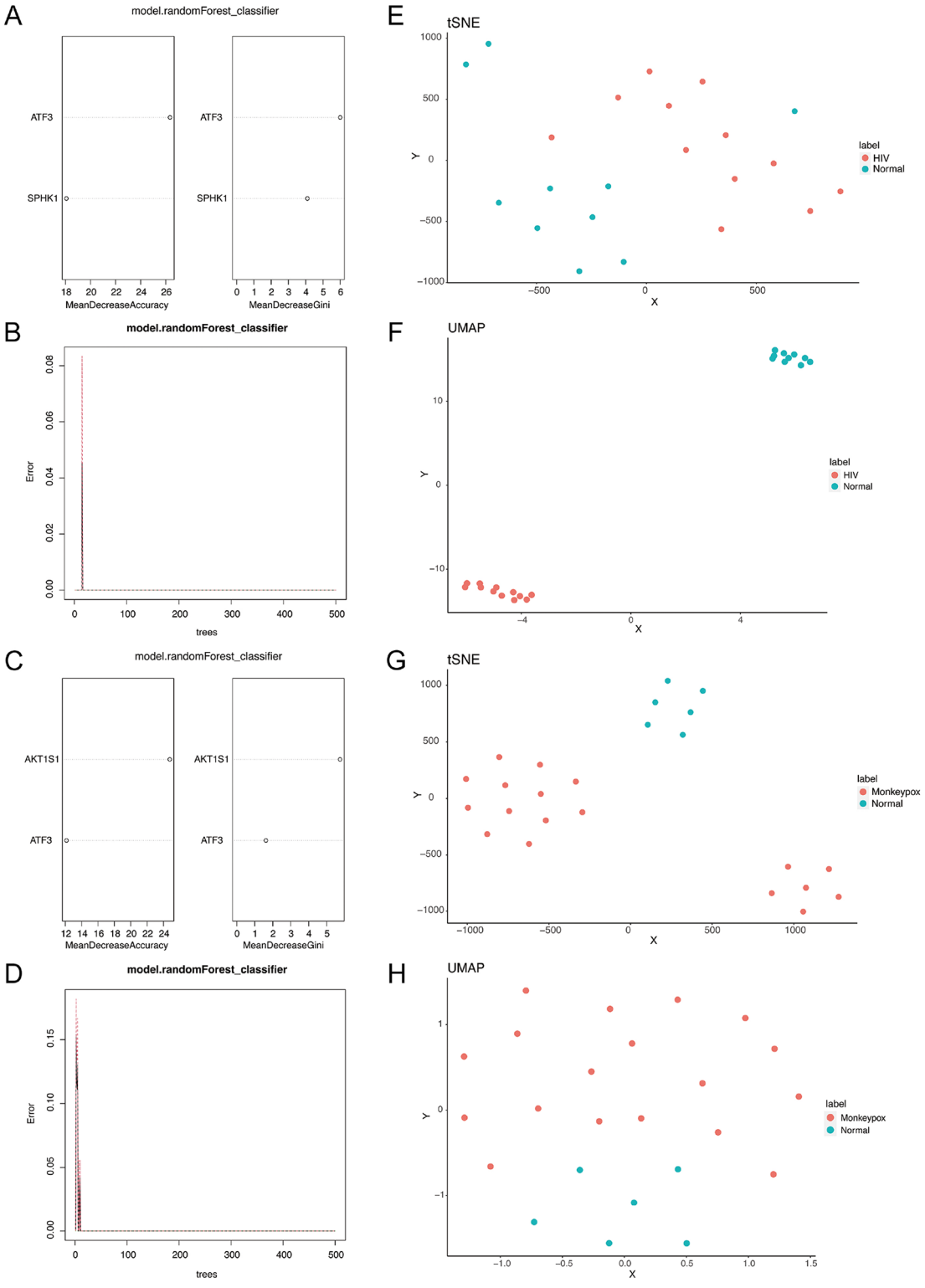

Figure 7. Machine learning (ML) screening of the key gene biomarkers. (A) Identification of ATF3 and SPHK1 as the most promising biomarkers using the random forest (RF) model, (B) with an excellent predictive accuracy for HIV outcomes. (C) Validation of ATF3 and AKT1S1 as the most promising biomarkers using the RF model, (D) with a remarkable predictive value in the MPXV data set. Significant trend distinction between the HIV and healthy samples observed using the (E) t-distributed stochastic neighbor embedding (tSNE) and the (F) uniform manifold approximation and projection (UMAP) model based on ATF3 and SPHK1 gene expression in the HIV data set. Significant separation of the MPXV and healthy samples using the (G) tSNE and (H) UMAP model based on ATF3 and AKT1S1 gene expression in the MPXV data set.

proteasome inhibitor MG-262, which regulates inflammatory and immune responses, reveals potential in reducing virus infection by inhibiting the NF-κB signaling pathway.[38] 8-Azaguanine (8-AG) is a well-known inhibitor of purine nucleotide biosynthesis implicated in anticancer and antiviral immunity.[39] Recent findings suggest that it serves as a potent suppressor of HIV-1 replication by altering another avenue of viral RNA processing.[40] GSK690693, a pan-AKT kinase

https://doi.org/10.1021/acsomega.3c07687
ACS Omega 2023, 8, 47283−47294

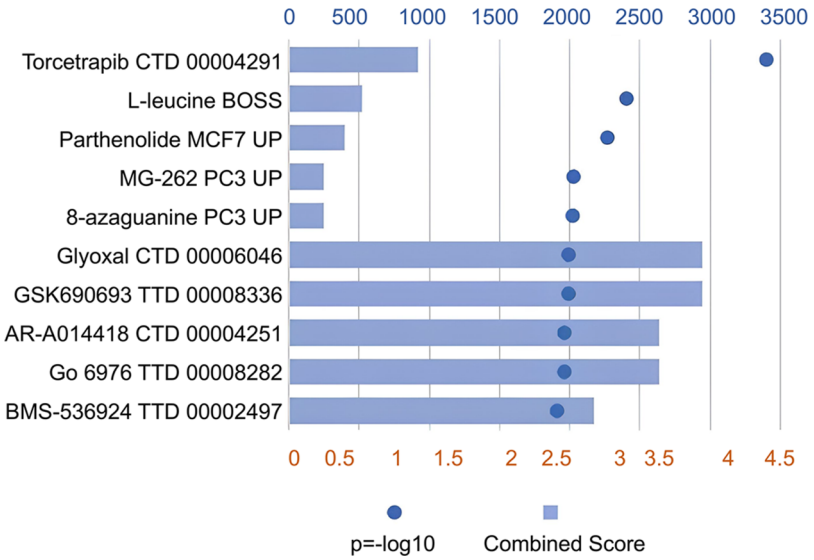

Figure 8. Top 10 potential therapeutic drug targets for the 5 key genes in the Drug Signatures database (DSigDB) on criteria of $p < 0.05$ and combined score >100.

inhibitor with potent antitumor and antivirus activity, exhibits excellent potential to decrease the secretion of chemokines and hyperinflammation in the pathogenesis of SARS-CoV-2.[41,42] The glycogen synthase kinase (GSK) inhibitor AR-A014418 has been found to be neuroprotective against HIV-associated neurotoxicity by mitigating HIV-associated procaspase induction, suggesting its potential as a therapeutic target for treatment of HIV-associated neurocognitive disorder.[43] While investigations into the clinical applications of these drugs in HIV and MPXV have been limited to date, the current study provided good insight into their possible therapeutic benefits. We hope that further investigation of their use will pave the way for innovative approaches to combat HIV and MPXV infections.

Despite the remarkable strength of our study, some limitations must be recognized in this work. First, our transcriptome data collected were limited to a single HIV and MPXV data set, which requires external validation to verify the results. Second, there is a lack of relevant patient data to validate our bioinformatics calculations. In addition, further investigation is necessary to explore the underlying mechanisms of our identified key genes and candidate drugs through fundamental experiments or clinical trials.

CONCLUSIONS

To summarize, our study revealed the shared pathogenesis linking HIV and MPXV skin infections. We identified pivotal biomarkers (SPRED1, SPHK1, ATF3, AKT3, and AKT1S1) and highlighted that multiple pathways, including the ERK cascade, NF-κB signaling, and various immune responses, played a collective role in the progression of both diseases. Our study provides a potential direction for evidence-based management strategies in HIV patients co-infected with MPXV.

MATERIALS AND METHODS

Microarray Data Sets. The transcriptome data were obtained from the Gene Expression Omnibus database (GEO, https://www.ncbi.nlm.nih.gov/geo/). The MPXV data set, identified as GSE219036, contained 9 samples of MPXV-infected keratinocytes, with 3 mock controls. The HIV data set contained skin samples from 6 HIV patients and 5 healthy donors, as outlined in GSE184320. Normalization of the gene expression data was performed for future analysis.

Characterization of Common DEGs in HIV and MPXV. We employed the criteria of |log FoldChange| ≥ 2 and $p < 0.05$ to identify DEGs using the "limma" R package. For the visualization of DEGs, we generated the volcano plots using the "volcano3D" R package. The common DEGs were screened by the Venn graph using Jvenn, a plug-in for the jQuery Javascript library.

Functional Annotation and Pathway Enrichment Analysis. To investigate the functional implications of the DEGs, gene ontology (GO) was performed by using the "clusterProfiler R" package to depict the DEGs in three levels: biological processes (BP), cellular components (CC), and molecular functions (MF). Kyoto Encyclopedia of Genes and Genomes (KEGG) enrichment was carried out using the database KOBAS (http://kobas.cbi.pku.edu.cn/genelist/). The statistical significance was determined using the False Discover Rate (FDR) < 0.05 and the count ≥ 2 thresholds. The results were graphically presented using the R package "ggplot2".

Identification of Hub Genes and Construction of Co-Expression Network. To create the PPI network, the common DEGs were uploaded to the STRING database (http://string-db.org/) for computational prediction of potential protein−protein interactions. The interactions were imported into Cytoscape (ver. 3.9.0) for visual representation. We then used a Cytoscape plug-in CytoHubba to determine the hub genes based on their nodes and interactions. Subsequently, we developed seven algorithms (Closeness, MCC, Degree, MNC, Radiality, Stress, and EPC) to identify the final hub genes, which were eventually depicted in a Venn diagram. For the visualization of the gene co-expression network, we uploaded the identified hub genes to the online database GeneMANIA (http://genemania.org), which enables the prediction of gene−gene interactions.

Analysis of Immune and Gene Correlation. Pearson's correlation analysis was implemented to evaluate the

https://doi.org/10.1021/acsomega.3c07687
ACS Omega 2023, 8, 47283−47294

correlations between the enrichment scores of the 16 distinct immune cell types and between the enrichment scores of the 13 immune pathways in both MPXV and HIV samples. In addition, a comprehensive analysis of the correlation coefficients between the 9 pivotal immune-related hub genes and individual immune cells and immune pathways was undertaken. The identified immune-related hub genes were defined as key genes for further investigation. The correlation between these identified key genes was subsequently analyzed by using Pearson's correlation. All correlational results were illustrated with the matrix diagram using the "corrplot" package in R. The graphic representation of individual gene expression in different samples was achieved by using radar plots generated by the "ggradar" R package.

Machine Learning Models. To conduct a further screening of the gene signature, we employed an ensemble of three ML algorithms including RF, tSNE, and UMAP. The optimization of parameters for these ML algorithms was achieved through a grid search conducted using the "POMA" package in R. We doubled our sample data to enhance the quality of our ML output. First, RF was used to screen biomarkers among the identified key genes. The RF classifier is a powerful ensemble ML algorithm that is built upon the addition of several decision tree layers, performed randomly on training data sets and subsets of features while splitting nodes. It is well known for its exceptional feature selection capability, even with high-dimensional features, and interpretability through the generation of optimized if−then rules at the end of the training process.[44] Subsequently, UMAP and tSNE were implemented to reduce the dimensionality and refine clusters based on the identified biomarkers through RF. UMAP is a nonlinear dimensionality reduction technique used to produce a low-dimensional projection of data, preserving local and global structures of data, along with reproducible and meaningful clusters.[45] Similarly, tSNE is used to replicate nonlinear mappings in the original data space to a lower dimension, allowing for structure identification at varying scales.[46]

Candidate Drug Prediction. We used the Drug Signatures database (DSigDB) in Enrichr to refine our candidate pharmacological molecules for the 5 key genes. Our selection criteria were a $p < 0.05$ and a combined score > 100. The result was presented graphically as column diagram using the "ggplot2" package in R.

Statistical Analysis. All results were processed with R software (version 4.1.2). The Benjamini−Hochberg method was applied for adjusted p value calculation. $P < 0.05$ was regarded as statistically significant.

■ ASSOCIATED CONTENT

Data Availability Statement

All transcriptome data are accessible in the public repository GEO (https://www.ncbi.nlm.nih.gov/geo/) and can be requested from the corresponding authors.

Supporting Information

The Supporting Information is available free of charge at https://pubs.acs.org/doi/10.1021/acsomega.3c07687.

Common DEGs between HIV and MPXV (Table S1); BP of GO analysis of the common DEGs (Table S2); CC of GO analysis of the common DEGs (Table S3); MF of GO analysis of the common DEGs (Table S4); KEGG analysis of the common DEGs (Table S5); and top 10 candidate drugs for potential combined therapy of HIV and MPXV (Table S6) (PDF)

■ AUTHOR INFORMATION

Corresponding Authors

Yuchen Cai − *Department of Plastic and Reconstructive Surgery, Shanghai Ninth People's Hospital, Shanghai Jiao Tong University School of Medicine, Shanghai 200011, China;* orcid.org/0000-0002-7536-906X; Email: 1917@sjtu.edu.cn

Jianda Zhou − *Department of Plastic Surgery, The Third Xiangya Hospital of Central South University, Changsha 410013, China;* orcid.org/0000-0002-3766-6573; Email: zhoujianda@csu.edu.cn

Authors

Xueyao Cai − *Department of Plastic Surgery, The Third Xiangya Hospital of Central South University, Changsha 410013, China*

Tianyi Zhou − *Department of Ophthalmology, Shanghai Ninth People's Hospital, Shanghai Jiao Tong University School of Medicine, Shanghai 200011, China; Shanghai Key Laboratory of Orbital Diseases and Ocular Oncology, Shanghai 200011, China*

Wenjun Shi − *Department of Plastic and Reconstructive Surgery, Shanghai Ninth People's Hospital, Shanghai Jiao Tong University School of Medicine, Shanghai 200011, China*

Complete contact information is available at: https://pubs.acs.org/10.1021/acsomega.3c07687

Author Contributions

⊥X.C. and T.Z. contributed equally. X.C.: conceptualization, methodology, and writing—original draft preparation. T.Z.: validation and formal analysis. W.S.: reviewing and editing the manuscript. Y.C.: methodology, reviewing and editing the manuscript, and supervision. J.Z.: supervision and project administration.

Funding

This work was supported by the Key Research and Development Projects in the Field of Social Development in Hunan Province (2020SK3030) and the Project of Science and Technology of Hunan Province No. 2021JJ40932.

Notes

The authors declare no competing financial interest.

■ ACKNOWLEDGMENTS

The authors express their sincere gratitude to the GEO database.

■ REFERENCES

(1) Rahimi, F.; Darvishi, M.; Talebi Bezmin Abadi, A. WHO Declared Monkeypox a Public-Health Emergency of International Concern: A Case for Prevention Rationale. *Int. J. Surg.* **2022**, *105*, No. 106850, DOI: 10.1016/j.ijsu.2022.106850.

(2) Mitjà, O.; Ogoina, D.; Titanji, B. K.; Galvan, C.; Muyembe, J.-J.; Marks, M.; Orkin, C. M. Monkeypox. *Lancet* **2023**, *401* (10370), 60−74.

(3) Huang, Y.; Mu, L.; Wang, W. Monkeypox: Epidemiology, Pathogenesis, Treatment and Prevention. *Signal Transduction Targeted Ther.* **2022**, *7* (1), 1−22, DOI: 10.1038/s41392-022-01215-4.

(4) Adler, H.; Gould, S.; Hine, P.; Snell, L. B.; Wong, W.; Houlihan, C. F.; Osborne, J. C.; Rampling, T.; Beadsworth, M. B.; Duncan, C. J.;

et al. Clinical Features and Management of Human Monkeypox: A Retrospective Observational Study in the UK. *Lancet Infect. Dis.* **2022**, *22* (8), 1153−1162.
(5) Huhn, G. D.; Bauer, A. M.; Yorita, K.; Graham, M. B.; Sejvar, J.; Likos, A.; Damon, I. K.; Reynolds, M. G.; Kuehnert, M. J. Clinical Characteristics of Human Monkeypox, and Risk Factors for Severe Disease. *Clin. Infect. Dis.* **2005**, *41* (12), 1742−1751.
(6) Angelo, K. M.; Smith, T.; Camprubí-Ferrer, D.; Balerdi-Sarasola, L.; Díaz Menéndez, M.; Servera-Negre, G.; Barkati, S.; Duvignaud, A.; Huber, K. L. B.; Chakravarti, A.; et al. Epidemiological and Clinical Characteristics of Patients with Monkeypox in the GeoSentinel Network: A Cross-Sectional Study. *Lancet Infect. Dis.* **2023**, *23* (2), 196−206.
(7) Tarín-Vicente, E. J.; Alemany, A.; Agud-Dios, M.; Ubals, M.; Suñer, C.; Antón, A.; Arando, M.; Arroyo-Andrés, J.; Calderón-Lozano, L.; Casañ, C.; et al. Clinical Presentation and Virological Assessment of Confirmed Human Monkeypox Virus Cases in Spain: A Prospective Observational Cohort Study. *Lancet* **2022**, *400* (10353), 661−669.
(8) Lucas, S.; Nelson, A. M. HIV and the Spectrum of Human Disease: HIV and the Spectrum of Human Disease. *J. Pathol.* **2015**, *235* (2), 229−241.
(9) Mitjà; Alemany, O.; Marks, A.; Lezama Mora, M.; Rodríguez-Aldama, J. I.; Torres Silva, J. C.; S, M.; Corral Herrera, E. A.; Crabtree-Ramirez, B.; Blanco, J. L.; Girometti, N.; et al. Mpox in People with Advanced HIV Infection: A Global Case Series. *Lancet* **2023**, *401* (10380), 939−949.
(10) Bhunu, C. P.; Mushayabasa, S.; Hyman, J. M. Modelling HIV/AIDS and Monkeypox Co-Infection. *Appl. Math. Comput.* **2012**, *218* (18), 9504−9518.
(11) Ogoina, D.; Iroezindu, M.; James, H. I.; Oladokun, R.; Yinka-Ogunleye, A.; Wakama, P.; Otike-odibi, B.; Usman, L. M.; Obazee, E.; Aruna, O.; Ihekweazu, C. Clinical Course and Outcome of Human Monkeypox in Nigeria. *Clin. Infect. Dis.* **2020**, *71* (8), e210−e214.
(12) Yoshimura, A.; Aki, D.; Ito, M. SOCS, SPRED, and NR4a: Negative Regulators of Cytokine Signaling and Transcription in Immune Tolerance. *Proc. Jpn. Acad., Ser. B* **2021**, *97* (6), 277−291, DOI: 10.2183/pjab.97.016.
(13) Suzuki, M.; Morita, R.; Hirata, Y.; Shichita, T.; Yoshimura, A. Spred1, a Suppressor of the Ras−ERK Pathway, Negatively Regulates Expansion and Function of Group 2 Innate Lymphoid Cells. *J. Immunol.* **2015**, *195* (3), 1273−1281.
(14) Pepini, T.; Gorbunova, E. E.; Gavrilovskaya, I. N.; Mackow, J. E.; Mackow, E. R. Andes Virus Regulation of Cellular microRNAs Contributes to Hantavirus-Induced Endothelial Cell Permeability. *J. Virol.* **2010**, *84* (22), 11929−11936.
(15) Ye, X.; Hemida, M. G.; Qiu, Y.; Hanson, P. J.; Zhang, H. M.; Yang, D. MiR-126 Promotes Coxsackievirus Replication by Mediating Cross-Talk of ERK1/2 and Wnt/β-Catenin Signal Pathways. *Cell. Mol. Life Sci.* **2013**, *70* (23), 4631−4644.
(16) Khoei, S. G.; Sadeghi, H.; Samadi, P.; Najafi, R.; Saidijam, M. Relationship between Sphk1/S1P and microRNAs in Human Cancers. *Biotechnol. Appl. Biochem.* **2021**, *68* (2), 279−287, DOI: 10.1002/bab.1922.
(17) Wolf, J. J.; Studstill, C. J.; Hahm, B. Emerging Connections of S1P-Metabolizing Enzymes with Host Defense and Immunity During Virus Infections. *Viruses* **2019**, *11* (12), 1097.
(18) Resop, R. S.; Bosque, A. Pharmacological Targeting of Sphingosine Kinases Impedes HIV-1 Infection of CD4 T Cells through SAMHD1Modulation. *J. Virol.* **2022**, *96* (9), No. e00096-22, DOI: 10.1128/jvi.00096-22.
(19) Ku, H.-C.; Cheng, C.-F. Master Regulator Activating Transcription Factor 3 (ATF3) in Metabolic Homeostasis and Cancer. *Front. Endocrinol.* **2020**, *11*, 556.
(20) Ashraf, U.; et al. Pathogenicity and Virulence of Japanese Encephalitis Virus: Neuroinflammation and Neuronal Cell Damage. *Virulence* **2021**, *12* (1), 968−980, DOI: 10.1080/21505594.2021.1899674.
(21) Shiromoto, F.; Aly, H. H.; Kudo, H.; Watashi, K.; Murayama, A.; Watanabe, N.; Zheng, X.; Kato, T.; Chayama, K.; Muramatsu, M.; Wakita, T. IL-1b/ATF3-Mediated Induction of Ski2 Expression Enhances Hepatitis B Virus x mRNA Degradation **2018** *503* 31854 1860.
(22) Henderson, A.; Holloway, A.; Reeves, R.; Tremethick, D. J. Recruitment of SWI/SNF to the Human Immunodeficiency Virus Type 1 Promoter. *Mol. Cell. Biol.* **2004**, *24* (1), 389−397.
(23) Wallace, V. C. J.; Blackbeard, J.; Pheby, T.; Segerdahl, A. R.; Davies, M.; Hasnie, F.; Hall, S.; McMahon, S. B.; Rice, A. S. C. Pharmacological, Behavioural and Mechanistic Analysis of HIV-1 Gp120 Induced Painful Neuropathy. *Pain* **2007**, *133* (1), 47−63.
(24) Vergadi, E.; Ieronymaki, E.; Lyroni, K.; Vaporidi, K.; Tsatsanis, C. Akt Signaling Pathway in Macrophage Activation and M1/M2 Polarization. *J. Immunol.* **2017**, *198* (3), 1006−1014.
(25) Tsiperson, V.; Gruber, R. C.; Goldberg, M. F.; Jordan, A.; Weinger, J. G.; Macian, F.; Shafit-Zagardo, B. Suppression of Inflammatory Responses during Myelin Oligodendrocyte Glycoprotein−Induced Experimental Autoimmune Encephalomyelitis Is Regulated by AKT3 Signaling. *J. Immunol.* **2013**, *190* (4), 1528−1539.
(26) Gangwani, M. R.; Noel, R. J.; Shah, A.; Rivera-Amill, V.; Kumar, A. Human Immunodeficiency Virus Type 1 Viral Protein R (Vpr) Induces CCL5 Expression in Astrocytes via PI3K and MAPK Signaling Pathways. *J. Neuroinflammation* **2013**, *10* (1), 902.
(27) Wojcechowskyj, J. A.; Lee, J. Y.; Seeholzer, S. H.; Doms, R. W. Quantitative Phosphoproteomics of CXCL12 (SDF-1) Signaling. *PLoS One* **2011**, *6* (9), No. e24918.
(28) Furler, R. L.; Uittenbogaart, C. H. Signaling through the P38 and ERK Pathways: A Common Link between HIV Replication and the Immune Response. *Immunol. Res.* **2010**, *48* (1−3), 99−109.
(29) Kang, Y.; Yu, Y.; Xu, S. Human Monkeypox Infection Threat: A Comprehensive Overview. *PLoS Negl. Trop. Dis.* **2023**, *17* (4), No. e0011246.
(30) Wong, L. M.; Jiang, G. NF-κB Sub-Pathways and HIV Cure: A Revisit. *EBioMedicine* **2021**, *63*, No. 103159.
(31) Nixon, C. C.; Mavigner, M.; Sampey, G. C.; Brooks, A. D.; Spagnuolo, R. A.; Irlbeck, D. M.; Mattingly, C.; Ho, P. T.; Schoof, N.; Cammon, C. G.; et al. Systemic HIV and SIV Latency Reversal via Non-Canonical NF-κB Signalling in Vivo. *Nature* **2020**, *578* (7793), 160−165.
(32) Wang, P.; Lu, P.; Qu, X.; Shen, Y.; Zeng, H.; Zhu, X.; Zhu, Y.; Li, X.; Wu, H.; Xu, J.; et al. Reactivation of HIV-1 from Latency by an Ingenol Derivative from Euphorbia Kansui. *Sci. Rep.* **2017**, *7* (1), No. 9451.
(33) Xuan, D. T. M.; Yeh, I.-J.; Wu, C.-C.; Su, C.-Y.; Liu, H.-L.; Chiao, C.-C.; Ku, S.-C.; Jiang, J.-Z.; Sun, Z.; Ta, H. D. K.; et al. Comparison of Transcriptomic Signatures between Monkeypox-Infected Monkey and Human Cell Lines. *J. Immunol. Res.* **2022**, *2022*, 1−17.
(34) Gupta, K. In Silico Structural and Functional Characterization of Hypothetical Proteins from Monkeypox Virus. *J. Genet. Eng. Biotechnol.* **2023**, *21* (1), 46.
(35) Onozato, T.; Nakamura, C. V.; Cortez, D. A. G.; Filho, B. P. D.; Ueda-Nakamura, T. *Tanacetum Vulgare* : Antiherpes Virus Activity of Crude Extract and the Purified Compound Parthenolide. *Phytother. Res.* **2009**, *23* (6), 791−796.
(36) Freund, R. R. A.; Gobrecht, P.; Fischer, D.; Arndt, H.-D. Advances in Chemistry and Bioactivity of Parthenolide. *Nat. Prod. Rep.* **2020**, *37* (4), 541−565.
(37) Ouled Aitouna, A.; Belghiti, Me.; Eşme, A.; Anouar, E.; Ouled Aitouna, A.; Zeroual, A.; Salah, M.; Chekroun, A.; Alaoui El Abdallaoui, H. E.; Benharref, A.; Mazoir, N. Chemical Reactivities and Molecular Docking Studies of Parthenolide with the Main Protease of HEP-G2 and SARS-CoV-2. *J. Mol. Struct.* **2021**, *1243*, No. 130705.
(38) Pujols, L.; Fernández-Bertolín, L.; Fuentes-Prado, M.; Alobid, I.; Roca-Ferrer, J.; Agell, N.; Mullol, J.; Picado, C. Proteasome Inhibition Reduces Proliferation, Collagen Expression, and Inflam-

matory Cytokine Production in Nasal Mucosa and Polyp Fibroblasts. *J. Pharmacol. Exp. Ther.* **2012**, *343* (1), 184−197.
(39) Kim, N.; Choi, J.-W.; Song, A. Y.; Choi, W. S.; Park, H.-R.; Park, S.; Kim, I.; Kim, H. S. Direct Potentiation of NK Cell Cytotoxicity by 8-Azaguanine with Potential Antineoplastic Activity. *Int. Immunopharmacol.* **2019**, *67*, 152−159.
(40) Wong, R. W.; Balachandran, A.; Haaland, M.; Stoilov, P.; Cochrane, A. Characterization of Novel Inhibitors of HIV-1 Replication That Function via Alteration of Viral RNA Processing and Rev Function. *Nucleic Acids Res.* **2013**, *41* (20), 9471−9483.
(41) Rhodes, N.; Heerding, D. A.; Duckett, D. R.; Eberwein, D. J.; Knick, V. B.; Lansing, T. J.; McConnell, R. T.; Gilmer, T. M.; Zhang, S.-Y.; Robell, K.; et al. Characterization of an Akt Kinase Inhibitor with Potent Pharmacodynamic and Antitumor Activity. *Cancer Res.* **2008**, *68* (7), 2366−2374.
(42) Callahan, V.; Hawks, S.; Crawford, M. A.; Lehman, C. W.; Morrison, H. A.; Ivester, H. M.; Akhrymuk, I.; Boghdeh, N.; Flor, R.; Finkielstein, C. V.; et al. The Pro-Inflammatory Chemokines CXCL9, CXCL10 and CXCL11 Are Upregulated Following SARS-CoV-2 Infection in an AKT-Dependent Manner. *Viruses* **2021**, *13* (6), 1062.
(43) Nguyen, T. B.; Lucero, G. R.; Chana, G.; Hult, B. J.; Tatro, E.; Masliah, E.; Grant, I.; Achim, C.; Everall, I. The Hiv Neurobehavioral Research Gr. Glycogen Synthase Kinase-3β (GSK-3β) Inhibitors AR-A014418 and B6B3O Prevent Human Immunodeficiency Virus-Mediated Neurotoxicity in Primary Human Neurons. *J. Neurovirol.* **2009**, *15*, 434−438, DOI: 10.1080/13550280903168131.
(44) Liu, Y.; Zhao, H. Variable Importance-Weighted Random Forests. *Quant. Biol.* **2017**, *5* (4), 338−351.
(45) Armstrong, G.; Martino, C.; Rahman, G.; Gonzalez, A.; Vázquez-Baeza, Y.; Mishne, G.; Knight, R. Uniform Manifold Approximation and Projection (UMAP) Reveals Composite Patterns and Resolves Visualization Artifacts in Microbiome Data. *mSystems* **2021**, *6* (5), No. e00691-21, DOI: 10.1128/mSystems.00691-21.
(46) Li, W.; Cerise, J. E.; Yang, Y.; Han, H. Application of T-SNE to Human Genetic Data. *J. Bioinform. Comput. Biol.* **2017**, *15* (04), No. 1750017.

https://doi.org/10.1021/acsomega.3c07687
ACS Omega 2023, 8, 47283−47294